

## Indium gallium zinc oxide layer used to decrease optical reflection loss at intermediate adhesive region for fabricating mechanical stacked multijunction solar cells

This content has been downloaded from IOPscience. Please scroll down to see the full text.

2017 Jpn. J. Appl. Phys. 56 012602

(<http://iopscience.iop.org/1347-4065/56/1/012602>)

View [the table of contents for this issue](#), or go to the [journal homepage](#) for more

Download details:

IP Address: 165.93.105.51

This content was downloaded on 19/12/2016 at 04:21

Please note that [terms and conditions apply](#).

You may also be interested in:

[Multi Junction Solar Cells Stacked with Transparent and Conductive Adhesive](#)

Toshiyuki Sameshima, Jun Takenezawa, Masahiko Hasumi et al.

[Activation of Silicon Implanted with Phosphorus and Boron Atoms by Infrared Semiconductor Laser Rapid Annealing](#)

Kan Ukawa, Yasushi Kanda, Toshiyuki Sameshima et al.

[Multi junction solar cells using band-gap induced cascaded light absorption](#)

Toshiyuki Sameshima, Hitomi Nomura, Shinya Yoshidomi et al.

[Evaluation of the junction interface of the crystalline germanium heterojunction solar cells](#)

Shinya Nakano, Yoshiaki Takeuchi, Tetsuya Kaneko et al.

[Application of n-type microcrystalline silicon oxide as back reflector of crystalline silicon heterojunction solar cells](#)

Kazuyoshi Nakada, Shinsuke Miyajima and Makoto Konagai

[Activation of silicon implanted with phosphorus and boron atoms by microwave annealing with carbon powder as a heat source](#)

Masahiko Hasumi, Tomohiko Nakamura, Shinya Yoshidomi et al.

[Photoinduced carrier annihilation in silicon pn junction](#)

Toshiyuki Sameshima, Takayuki Motoki, Keisuke Yasuda et al.

[Studying nanostructured nipple arrays of moth eye facets helps to design better thin film solar cells](#)

Rahul Dewan, Stefan Fischer, V Benno Meyer-Rochow et al.



# Indium gallium zinc oxide layer used to decrease optical reflection loss at intermediate adhesive region for fabricating mechanical stacked multijunction solar cells

Toshiyuki Sameshima\*, Takeshi Nimura, Takashi Sugawara, Yoshihiro Ogawa, Shinya Yoshidomi, Shunsuke Kimura, and Masahiko Hasumi

Tokyo University of Agriculture and Technology, Koganei, Tokyo 184-8588, Japan

\*E-mail: tsamesim@cc.tuat.ac.jp

Received July 20, 2016; accepted October 1, 2016; published online December 6, 2016

Reduction of optical reflection loss is discussed in three mechanical stacked samples: top crystalline silicon and bottom crystalline germanium substrates, top crystalline GaAs and bottom crystalline silicon substrates, and top crystalline GaP and bottom crystalline silicon substrates using an epoxy-type adhesive with a reflective index of 1.47. Transparent conductive Indium gallium zinc oxide (IGZO) layers with a refractive index of 1.85 were used as antireflection layers. IGZO layers were formed on the bottom surface of the top substrate and the top surface of the bottom substrate of the three stacked samples with thicknesses of 188, 130, and 102 nm. The insertion of IGZO layers decreased the optical reflectivity of the stacked samples. The IGZO layers provided high effective optical absorbency of bottom substrates of 0.925, 0.943, and 0.931, respectively, for light wavelength regions for light in which the top substrates were transparent and the bottom substrates were opaque.

© 2017 The Japan Society of Applied Physics

## 1. Introduction

Semiconductor solar cells are important devices, which produce electrical power directly from sunlight.<sup>1–5</sup> It has been widely investigated as clean energy sources. The conversion efficiency  $E_{\text{ff}}$  of a single solar cell is governed by the height of built-in potential and light absorption characteristic, which depend on the band gap of the semiconductor.  $E_{\text{ff}}$  is strictly limited by 32.7%, which is called the Shockley–Queisser limit.<sup>1</sup> To overcome the  $E_{\text{ff}}$  limitation of a single solar cell and realize a higher  $E_{\text{ff}}$ , a multijunction solar cell has been proposed.<sup>6–16</sup> A combination of solar cells with different band gaps effectively absorb sunlight from ultraviolet to infrared wavelength regions. Solar cells ohmically connected cooperatively increase the open circuit voltage  $V_{\text{OC}}$ . A three-junction solar cell InGaP/GaAs/Ge with  $E_{\text{ff}}$  of 31.5% fabricated by the epitaxial crystalline growth method has been reported.<sup>14</sup> Mechanically stacked multijunction solar cells have also been reported.<sup>12,17–23</sup> The mechanical stacking method of individual solar cells allows a wide selection of semiconductor materials such as amorphous, polycrystalline, and organic semiconductors as well as single-crystalline inorganic semiconductors. Moreover, this method makes it possible to fabricate large size solar cells. We have proposed a processing method of mechanically stacking semiconductor solar cells with a transparent conductive adhesive dispersed with indium–tin–oxide (ITO) conductive particles.<sup>23–26</sup> A connecting resistivity lower than  $1.0 \Omega \text{cm}^2$  has been achieved.<sup>26</sup> It was low enough to fabricate multijunction solar cells with  $E_{\text{ff}}$  higher than 30%.

There is a still serious problem of optical reflection loss at the intermediate adhesive interface region. Semiconductor materials have high refractive indices in general because of their strong covalent bonding, while an organic adhesive has a low refractive index. A large difference in refractive index causes high optical reflection, which reduces the transmittance of light and the photoinduced current density into the bottom cell. Optical reflection loss at the intermediate adhesive interface should be reduced to maintain the current matching condition between the top and bottom cells, which

is an important condition to achieve a high  $E_{\text{ff}}$ .<sup>13,14</sup> We proposed the use of transparent conductive indium gallium zinc oxide (IGZO) as the optical antireflection layer at the interfaces of the semiconductor and the adhesive to reduce optical reflection loss.<sup>27</sup> IGZO has been widely used as the active layer in thin-film transistors, which have been applied in the switching element of active-matrix-flat panel displays.<sup>28–30</sup> The technology of film formation on meter-sized large substrates by the plasma sputtering method has been established. The technology of control of electrical resistivity has also been developed.<sup>29</sup> IGZO layers have the anti-reflection effect because its refractive index of 1.85 was lower than that (3.5) of silicon and higher than that of epoxy adhesive.<sup>31,32</sup> We reported the increase in transmissivity in the infrared region for the silicon-stacked samples with a structure of Si/IGZO/adhesive/IGZO/Si.<sup>27</sup> However, the reduction characteristics in optical reflectivity has not been experimentally demonstrated yet in stacked samples with different materials with different band gaps.

In this paper, we report the experimental demonstration of reduction of optical reflection loss using IGZO layers at the intermediate adhesive region at wavelength ranging from the visible to infrared region, which is an important region for solar cells. We use three kinds of stacked samples with different material substrates: top crystalline silicon and bottom crystalline germanium, top crystalline GaAs and bottom silicon, and top crystalline GaP and bottom silicon to discuss optical reflectivity properties. Two IGZO layers are used at the bottom interface of the top substrate and the top interface of the bottom substrate in the intermediate adhesive region. We demonstrate the decrease in the optical reflectivity of all the stacked samples with IGZO layers but not in the controlled stacked sample without IGZO layers. We introduce the effective optical absorbency  $A_{\text{eff}}$  of the bottom substrate. We report  $A_{\text{eff}}$  values higher than 0.9 for three kinds of samples with IGZO anti-reflection layers with appropriate thicknesses.

## 2. Experimental procedure

In order to fabricate stacked samples as shown in Fig. 1,

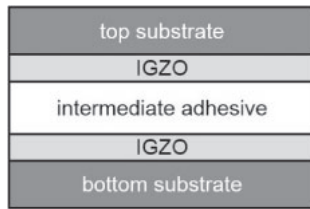


**Fig. 1.** Sample structure of stacked top and bottom substrates with IGZO anti-reflection layers and intermediate adhesive.

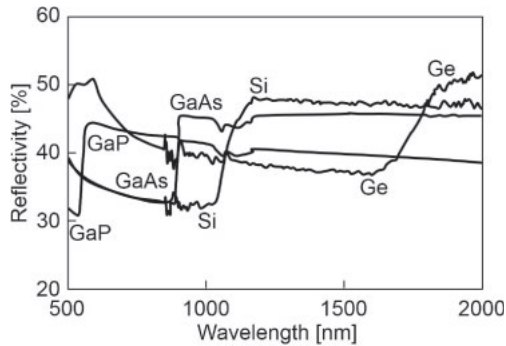


**Fig. 2.** Experimental reflectivity spectra of crystalline germanium, silicon, GaAs, and GaP substrates.

we prepared four kinds of single-crystalline semiconductor substrates of 500- $\mu\text{m}$ -thick p-type 10  $\Omega\text{cm}$  (100) germanium, 500- $\mu\text{m}$ -thick n-type 17  $\Omega\text{cm}$  (100) silicon, 500- $\mu\text{m}$ -thick n-type 20  $\Omega\text{cm}$  (100) GaAs, and 500- $\mu\text{m}$ -thick n-type 5  $\Omega\text{cm}$  (100) GaP. Figure 2 shows the experimental reflectivity spectra of crystalline germanium, silicon, GaAs, and GaP described above. The experimental optical reflectivity of the 500- $\mu\text{m}$ -thick crystalline germanium substrate decreased from 51 to 37% as the wavelength increased from 582 to 1600 nm. The photon energy in that wavelength region was higher than the indirect band gap of 0.67 eV of crystalline germanium. The 500- $\mu\text{m}$ -thick crystalline germanium substrate was completely opaque at wavelengths lower than 1600 nm because the optical penetration depth determined by the extinction coefficient shown in Fig. 3(b)<sup>33)</sup> was much lower than the thickness of the substrate. Light was completely absorbed in the crystalline germanium substrate at wavelengths lower than 1600 nm. The optical reflectivity of the crystalline germanium substrate was determined only by the reflectivity of the top surface of crystalline germanium depending on the refractive index and extinction coefficient shown in Figs. 3(a) and 3(b) at wavelengths lower than 1600 nm. The low optical reflectivity of 37% at 1600 nm was due to the low reflective index and extinction coefficient. On the other hand, the experimental optical reflectivity gradually increased from 37 to 51% as the wavelength increased from 1600 to 1900 nm, as shown in Fig. 2 because the substrate becomes gradually transparent and the light reflected at the bottom surface comes back to the top surface. Multiple reflections between the top and bottom surfaces increases the optical reflectivity of the crystalline germanium substrate. Similar characteristics of the experimentally optical reflectivity were observed in the cases of crystalline silicon, crystalline GaAs, and crystalline GaP, as shown in Fig. 2. They clearly depend on their own band gap energies of 1.1, 1.43,

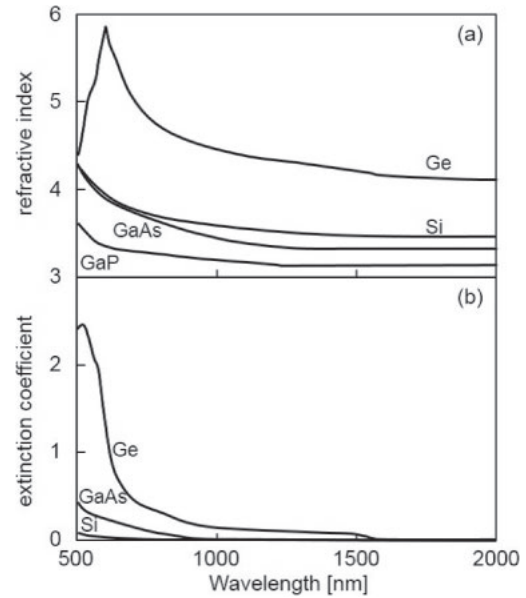


**Fig. 3.** (a) Refractive index and (b) extinction coefficient of crystalline germanium, crystalline silicon, crystalline GaAs, and crystalline GaP.<sup>33)</sup> The extinction coefficient of crystalline GaP was negligible small.

and 2.26 eV for crystalline silicon, crystalline GaAs, and crystalline GaP, respectively. The light wavelength just before the experimentally optical reflectivity increased (1600 nm for crystalline germanium given above) were 1020, 880, and 540 nm for crystalline silicon, crystalline GaAs, and crystalline GaP, respectively. The samples were opaque and the light is completely absorbed at wavelengths less than above values. The experimentally optical reflectivity increased from 32.5 to 48% as the wavelength increased from 1020 to 1150 nm for the crystalline silicon substrate. It increased from 32.5 to 45.5% as the wavelength increased from 880 to 902 nm for the crystalline GaAs substrate. It increased from 31.3 to 44.3% as the wavelength increased from 540 to 568 nm for the crystalline GaP substrate. These increases in optical reflectivity were caused by the multiple reflections between the top and bottom surfaces because the crystalline substrates became transparent as the wavelength increased, similar to the case of the crystalline germanium substrates. Figure 2 shows the wavelength region to be discussed in this paper, in which the top substrate is transparent and the bottom substrate is opaque. The shortest wavelength  $\lambda_1$  and the longest wavelength  $\lambda_2$  in this wavelength region for samples with combinations of different materials are given as Table I.

IGZO films were formed on the semiconductor surfaces by radio-frequency Ar plasma sputtering at 2000 W with  $\text{In}_{1.0}\text{Ga}_{1.2}\text{Zn}_{1.0}\text{O}_{1.4}$  as the target at room temperature. The optimum thickness of IGZO for reducing the optical reflectivity at wavelengths between  $\lambda_1$  and  $\lambda_2$  was determined using a calculation program to be discussed in Sect. 3. The optical reflectivity spectra of the IGZO/semiconductor samples were measured using a spectrometer. The film thickness was estimated by best fitting calculated spectra using a program including the optical interfere effect with film thickness to the experimental spectra.<sup>27)</sup> By analyzing optical spectra, we determined the experimental thicknesses of the IGZO layer ( $d_{\text{ex}}$ ) to 188 nm in stacked GaAs and silicon, 130 nm in

**Table I.** Lists of materials for fabricating stacked samples,  $\lambda_1$ ,  $\lambda_2$ ,  $\lambda_{\text{eff}}$ ,  $d_{\text{cal}}$ , and  $d_{\text{ex}}$ .  $\lambda_1$  and  $\lambda_2$  are determined from Fig. 2 as the shortest and longest wavelengths for conditions with transparent top and opaque bottom substrates (in nm).  $d_{\text{cal}}$  is given by the maximum calculated  $A_{\text{eff}}$ .  $d_{\text{ex}}$  is the experimental thickness of the IGZO layer.  $\lambda_{\text{eff}}$  is given by  $d_{\text{cal}}$  as the effective best anti-reflection wavelength.

Sample	$\lambda_1$	$\lambda_2$	$\lambda_{\text{eff}}$	$d_{\text{cal}}$	$d_{\text{ex}}$
Si/Ge	1150	1600	1356	183	188
GaAs/Si	902	1020	959	130	130
GaP/Si	568	1020	761	102	102

stacked GaAs and silicon, and 102 nm in stacked GaP and silicon, as listed in Table I. The IGZO layers formed on the semiconductor substrates were heated at 350 °C in air atmosphere for 1 h to decrease the density of free carriers and prevent serious free carrier absorption in the infrared region in stacked silicon and germanium. Heating at 350 °C for 1 h increased the resistivity of the IGZO layer from 0.0011 to 0.056  $\Omega$  cm, whose connecting resistivity was  $1.1 \times 10^{-6}$   $\Omega$  cm<sup>2</sup>, which is much lower than 1.0  $\Omega$  cm<sup>2</sup>.<sup>34-40</sup> On the other hand, the IGZO film with 0.056  $\Omega$  cm only causes a very small free carrier absorption with an absorption coefficient of 0.2 cm<sup>-1</sup> and an extinction coefficient of  $2.7 \times 10^{-6}$  at the longest  $\lambda_2$  of 1600 nm, as shown in Table I, which is in accordance with the free carrier absorption theory.<sup>34,41-43</sup> IGZO layers are therefore optically transparent and electrically conductive. A transparent epoxy prepolymer and hardener gels were prepared. They were mixed and diluted with xylene. 20- $\mu$ m-diameter ITO particles were then dispersed at 6 wt % (1 vol %) in the gels. The adhesive with ITO particles was pasted on the surfaces of the bottom substrates. The top substrate was placed on the adhesive. The samples were then kept for 1.5 h at RT in 0.8 MPa N<sub>2</sub> atmosphere to solidify the epoxy adhesive. These were our conventional stacking conditions for realizing connecting resistivities lower than 1.0  $\Omega$  cm<sup>2</sup>. High optical transmissivity was confirmed at wavelengths from 500 to 2000 nm by measuring transmissivity spectra of ITO diffused epoxy adhesive sandwiched by two quartz substrates. Transmissivity analysis showed refractive index of the adhesive ranging from 1.44 to

1.5. The distribution of the refractive indices probably resulted from incorporation of small air bubbles during ITO particle dispersion into the adhesive. We set the average refractive index of the adhesive to be 1.47 for the analysis of the present results. Stacked samples were consequently fabricated with structures of Si/IGZO/adhesive/IGZO/Ge, GaAs/IGZO/adhesive/IGZO/Si, and GaP/IGZO/adhesive/IGZO/Si. Moreover, samples with structures of Si/adhesive/Ge, GaAs/adhesive/Si, and GaP/adhesive/Si were also fabricated as the control samples. The optical reflectivity spectra of the stacked samples were measured using a spectrometer in the case of light illumination to the top surface of the samples.

### 3. Calculation

A numerical calculation program of optical reflectivity spectra was developed to analyze experimental reflectivity spectra and  $A_{\text{eff}}$ .<sup>27,34,41-43</sup> The sample structure shown in Fig. 1 was set for calculation. The data of the refractive index  $n$  and extinction coefficient  $k$ <sup>33</sup> shown in Fig. 3 are used. The top and bottom substrates were thick enough to ignore the optical interference effect of incident incoherent light. The intermediate adhesive layer has a thickness of about 20  $\mu$ m in reality. We also assumed that no optical interference effect occurred between the top and bottom adhesive surfaces. The Fresnel-type optical interference effect was calculated for the IGZO layer assuming a simple plain wave model.<sup>41-44</sup> The optical phase coupling results in an interface with a new reflectivity coefficient depending on the IGZO film thickness for both surfaces of the intermediate adhesive layer. Their reflectivity is given by the absolute squared reflectivity coefficient. The four individual optical interfaces are therefore formed by five optical media of air, top substrate, intermediate adhesive layer, bottom substrate, and air, as shown in Fig. 4, while the real sample has six material interfaces, as shown in Fig. 1. A calculation system for scalar-type multiple reflections and transmission was prepared with an incident angle of 0 between the four interfaces, as shown in Fig. 4, to obtain optical reflectivity, which includes many reflectivity components. The extinction coefficient  $k$  also gives the reduction in light intensity by  $\exp(-4\pi kx/\lambda)$  when

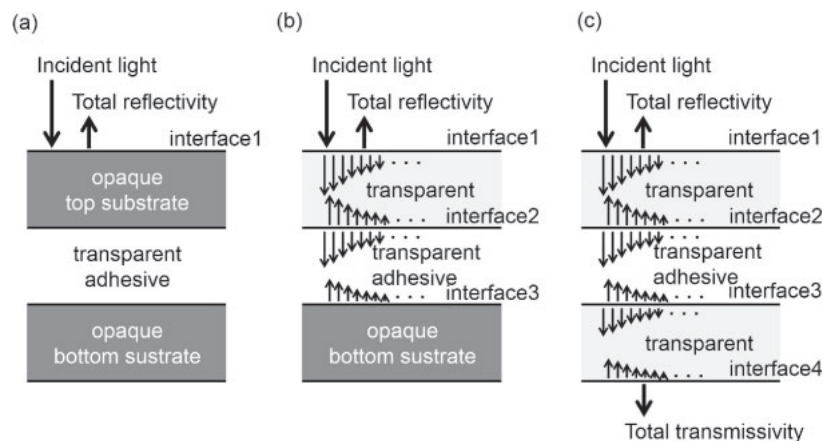


**Fig. 4.** Calculation illustrations of scalar-type multiple reflections and transmission with an incident angle of 0 between the four interfaces of air/top substrate, top substrate/adhesive, adhesive/bottom substrate, and bottom substrate/air. The reflectivity of the top substrate/adhesive, and adhesive/bottom substrate was due to the IGZO optical interference effect. Panels (a), (b), and (c) show calculation illustrations for wavelengths much lower than  $\lambda_1$  ( $\lambda \ll \lambda_1$ ), between  $\lambda_1$  and  $\lambda_2$  ( $\lambda_1 < \lambda < \lambda_2$ ), and higher than  $\lambda_2$  ( $\lambda > \lambda_2$ ).

light propagates for a distance of  $x$  at  $\lambda$ . There are four important properties. 1) When the wavelength is much shorter than  $\lambda_1$ , the top substrate is opaque. The optical reflectivity of a sample is determined by the reflectivity of the first interface between air and the top substrate, as shown in Fig. 4(a). 2) When the wavelength is near  $\lambda_1$ , the top substrate becomes partially transparent. The optical reflectivity of the sample includes multiple reflection components between the three top interfaces as well as a component given by the top surface. 3) When the wavelength is located between  $\lambda_1$  and  $\lambda_2$ , the top substrate is transparent and the bottom substrate is still opaque. The optical reflectivity of the sample is given by multiple reflection components between the three top interfaces as well as a component given by the top surface, as shown in Fig. 4(b). The reflectivity at second and third interfaces given by IGZO is therefore important to reduce the total reflectivity. 4) When the wavelength is longer than  $\lambda_2$ , the bottom substrate becomes finally transparent. Multiple reflections between all the four interfaces contribute to the optical reflectivity of the sample as well as a component given by the top surface, as shown in Fig. 4(c).

To estimate optical reflection loss, the effective optical absorptency  $A_{\text{eff}}$  was defined as

$$A_{\text{eff}} = \frac{\int_{\lambda_1}^{\lambda_2} [100 - R_s(\lambda)] d\lambda}{\int_{\lambda_1}^{\lambda_2} [100 - r(\lambda)] d\lambda}, \quad (1)$$

where  $R_s(\lambda)$  is the optical reflectivity (%) of the sample at the wavelength  $\lambda$ , and  $r(\lambda)$  is the reflectivity (%) at the top surface of an individual top substrate. The denominator is the integration of light incidence ratio into the top substrate between  $\lambda_1$  and  $\lambda_2$  because the top substrate was transparent between  $\lambda_1$  and  $\lambda_2$ . The numerator is the integration of the optical absorption ratio of the sample between  $\lambda_1$  and  $\lambda_2$ . Because the bottom substrate was opaque between  $\lambda_1$  and  $\lambda_2$ , the numerator of Eq. (1) depends on the optical reflectivity at the interface adhesive layer.  $A_{\text{eff}}$  therefore gives the effective optical absorptency of the bottom substrate of incident light at the top substrate. The optical reflection loss ratio of the intermediate adhesive layer between  $\lambda_1$  and  $\lambda_2$  is therefore given by  $1 - A_{\text{eff}}$ .  $A_{\text{eff}}$  was calculated with different thicknesses of the IGZO layer using the calculation program given above. For sample fabrication, the thickness of the IGZO layer  $d_{\text{cal}}$  was determined by the maximum calculated  $A_{\text{eff}}$ . The values of  $d_{\text{cal}}$  were 183 nm in stacked silicon and germanium, 130 nm in stacked GaAs and silicon, and 102 nm in stacked GaP and silicon, respectively.  $d_{\text{cal}}$  gives the effective wavelength  $\lambda_{\text{eff}}$  and the phase difference  $\phi$  of incident plain wave of light at a wavelength  $\lambda_{\text{eff}}$  between the top and bottom surface of IGZO for the best anti-reflection condition as

$$\lambda_{\text{eff}} = 4nd_{\text{cal}}, \quad (2a)$$

$$\phi = \frac{2\pi}{\lambda_{\text{eff}}} nd_{\text{cal}} = \frac{\pi}{2}, \quad (2b)$$

where  $n$  is the refractive index of the IGZO layer. The value of  $\lambda_{\text{eff}}$  was between  $\lambda_1$  and  $\lambda_2$  and slightly lower than the middle point of  $\lambda_1$  and  $\lambda_2$ , as shown in Table I for each sample.

The experimental  $A_{\text{eff}}$  values of the stacked samples were also obtained from the experimentally obtained optical reflectivity spectra.  $r(\lambda)$  is determined using the experimental

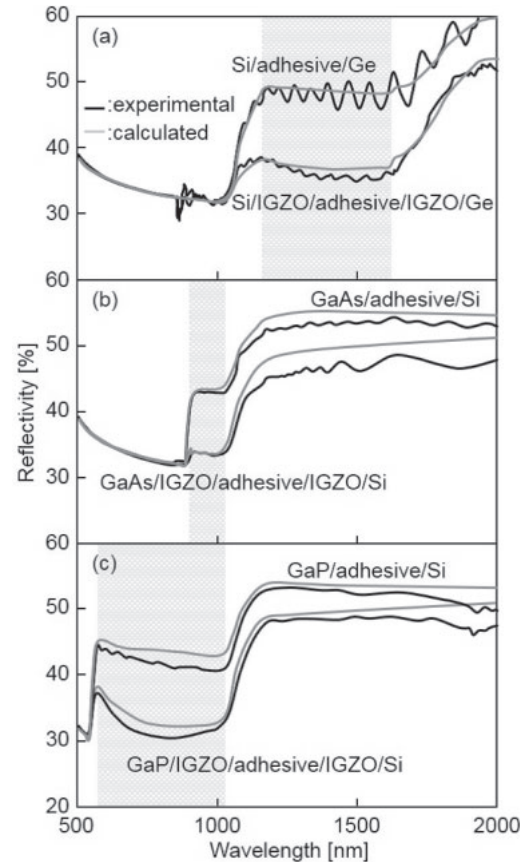


**Fig. 5.** Experimental and calculated optical reflectivity spectra of samples with structures of (a) Si/IGZO/adhesive/IGZO/Ge and Si/adhesive/Ge, (b) GaAs/IGZO/adhesive/IGZO/Si and GaAs/adhesive/Si, and (c) GaP/IGZO/adhesive/IGZO/Si and GaP/adhesive/Si. The hatched areas show wavelength regions between  $\lambda_1$  and  $\lambda_2$  given in Table I.

optical reflectivity (%)  $R_{\text{top}}(\lambda)$  of the individual top substrate shown in Fig. 2.  $R_{\text{top}}(\lambda)$  is given by the contribution of scalar-type multiple reflections at the top and bottom surfaces as

$$\begin{aligned} \frac{R_{\text{top}}(\lambda)}{100} &= \frac{r(\lambda)}{100} + \left[1 - \frac{r(\lambda)}{100}\right]^2 \left\{ \frac{r(\lambda)}{100} + \left[\frac{r(\lambda)}{100}\right]^3 + \dots \right\} \\ &= \frac{2r(\lambda)}{100 + r(\lambda)}. \end{aligned} \quad (3a)$$

$r(\lambda)$  is therefore given by  $R_{\text{top}}(\lambda)$  as

$$r(\lambda) = \frac{100 \times R_{\text{top}}(\lambda)}{200 - R_{\text{top}}(\lambda)}. \quad (3b)$$

#### 4. Results and discussion

Figure 5 shows the optical reflectivity spectra of the samples with structures of (a) Si/IGZO/adhesive/IGZO/Ge and Si/adhesive/Ge, (b) GaAs/IGZO/adhesive/IGZO/Si and GaAs/adhesive/Si, and (c) GaP/IGZO/adhesive/IGZO/Si and GaP/adhesive/Si. The hatched areas show wavelength regions ranging from  $\lambda_1$  to  $\lambda_2$  given in Table I each figure, in which the top substrate is transparent and the bottom substrate is opaque. Light coming in the top surface can partially reflect at the intermediate adhesive region and comes back to the top surface. The optical reflectivity measurement at the top surface therefore gives the degree of optical reflection at the intermediate adhesive region. The sample with 188-nm-thick IGZO layers formed on the bottom surface of the silicon

substrate and the top surface of germanium substrate showed an optical reflectivity of 38.6% at 1150 nm. The optical reflectivity gradually decreased to 36.4% as the wavelength increased to 1600 nm. At a low optical reflectivity, it is clearly demonstrated that the IGZO layer showed the anti-reflection effect. Light was effectively transmitted from silicon to germanium with no substantial light reflection at the intermediate adhesive region. On the other hand, the control sample, Si/adhesive/Ge, showed a high optical reflectivity between 46.7 and 50.2% at wavelengths ranging from 1150 to 1600 nm. The high optical reflectivity resulted from substantial reflections at the interfaces between silicon and the adhesive and between the adhesive and germanium. Figure 5(a) also shows the calculated optical reflectivity spectra of samples with structures of Si/188-nm-thick IGZO/adhesive/188-nm-thick IGZO/Ge and Si/adhesive/Ge in gray curves. The calculated spectra showed characteristics similar to the experimental spectra over the wavelength region from 500 to 2000 including the region ranging from  $\lambda_1$  (1150 nm) to  $\lambda_2$  (1600 nm). The optical reflectivities of four cases of experimental and calculated spectra were almost the same. They decreased as the wavelength increased up to 1000 nm. This clearly shows that the experimentally optical reflectivity was determined by the reflectivity of the top surface of the crystalline silicon substrate. The optical reflectivity increased as the wavelength increased from 1000 nm. The good agreement among experimental and calculated values between 1150 and 1600 nm indicates that the optical reflectivity resulted from the effect multiple reflections among the top surface of crystalline silicon, the silicon/adhesive interface, and the adhesive/crystalline germanium interface. The calculation model of the anti-reflection effect of the sample with IGZO well explains the experimental result of low optical reflectivity between 1150 and 1600 nm, while the calculated spectrum also explains the experimental result of high optical reflectivity with no anti-reflection effect of the control sample of Si/adhesive/Ge. When the wavelength increased from 1600 nm, the optical reflectivity further increased for both stacked samples. The good agreement between experimental and calculated values indicates that optical reflectivity resulted from the effect of multiple reflections among the top surface of crystalline silicon, the silicon/adhesive interface, the adhesive/crystalline germanium interface, and the bottom surface of crystalline germanium because of the transparency of crystalline germanium. Small fringes were observed in experimental spectra. There are possibilities of the partial optical interference effect between the top and bottom surfaces of the adhesive, and the two-dimensional Fresnel diffraction caused by surface roughness at the adhesive layer.

The sample with 130-nm-thick IGZO layers formed on the bottom surface of the GaAs substrate and the top surface of the silicon substrate showed optical reflectivities ranging from 33.4 to 33.9% between 902 and 1020 nm, as shown in Fig. 5(b). These low optical reflectivities demonstrate that IGZO layer has the anti-reflection effect in the short wavelength region. Light effectively transmitted from GaAs to silicon with no substantial light reflection at the intermediate adhesive region. On the other hand, the control sample with GaAs/adhesive/Si showed high optical reflectivities between 40.1 and 42.3% at wavelengths ranging from 902 to 1020 nm.

These high optical reflectivities were due to substantial optical reflection at the intermediate adhesive region. Calculated optical reflectivity spectra shown by gray curves agreed well with the experimental spectra of samples with the structures of GaAs/130-nm-thick IGZO/adhesive/130-nm-thick IGZO/Si and Si/adhesive/Ge at wavelengths ranging from 902 to 1020 nm. The optical reflectivities for four cases of experimental and calculated spectra were almost the same. They decreased as the wavelength increased up to 890 nm. This clearly shows that the experimental optical reflectivity was determined by the reflectivity of the top surface of the crystalline GaAs substrate. The optical reflectivity increased as the wavelength increased from 890 nm. The good agreement among experimental and calculated values between 902 to 1020 nm indicates that optical reflectivity was due to the effect of multiple reflections among the top surface of crystalline GaAs, the GaAs/adhesive interface, and adhesive/crystalline silicon interface. The calculation model of the anti-reflection effect of IGZO well explains the low experimental optical reflectivities ranging from 902 to 1020 nm, while the calculated spectrum also explains the high experimental optical reflectivity with no anti-reflection effect of the control sample of GaAs/adhesive/Si. When the wavelength increased from 1020 nm, the optical reflectivity further increased for both stacked samples. The similar properties between experimental and calculated values indicate that optical reflectivity resulted from the effect of multiple reflections among the top surface of crystalline GaAs, the crystalline GaAs/adhesive interface, the adhesive/crystalline silicon interface, and the bottom surface of crystalline silicon because of the transparency of crystalline silicon. The calculation model of the antireflection effect of IGZO was demonstrated in the case of stacking GaAs and Si.

The sample with 102-nm-thick IGZO layers formed on the bottom surface of the GaP substrate and the top surface of the silicon substrate showed an optical reflectivity of 35.6% at 568 nm. The optical reflectivity decreased to 32.5% as the wavelength increased to 1020 nm, as shown in Fig. 5(c). Light effectively transmitted from GaP to silicon with no substantial light reflection at the intermediate adhesive region. On the other hand, the sample with GaP/adhesive/Si showed a high optical reflectivity between 44.4 and 41.0% at wavelengths ranging from 568 to 1020 nm. The high optical reflectivity was due to substantial optical reflection at the intermediate adhesive region. The calculated optical reflectivity spectra were similar to the experimental spectra for samples with the structures of GaP/102-nm-thick IGZO/adhesive/102-nm-thick IGZO/Si, and GaP/adhesive/Si. The Similarities between experimental and calculated values indicate that the optical reflectivity was due to the effect of multiple reflections among the top surface of crystalline GaP, the crystalline GaP/adhesive interface and the adhesive/crystalline silicon interface. The calculation model of the anti-reflection effect of IGZO well explains the low experimental optical reflectivity from 568 to 1020 nm, while the calculated spectrum also explains the high experimental optical reflectivity with no anti-reflection effect in the control sample of GaP/adhesive/Si. When the wavelength increased from 1020 nm, the optical reflectivity further increased for both stacked samples. Similarities between experimental and calculated values indicate that optical reflectivity results from

**Table II.** Experimental  $A_{\text{eff}}$  given in Eq. (1).

Sample	$A_{\text{eff}}$
Si/188 nm IGZO/adhesive/188 nm IGZO/Ge	0.925
GaAs/130 nm IGZO/adhesive/130 nm IGZO/Si	0.943
GaP/102 nm IGZO/adhesive/102 nm IGZO/Si	0.931
Si/adhesive/Ge	0.751
GaAs/adhesive/Si	0.811
GaP/adhesive/Si	0.796

the multiple reflection effect among the top surface of crystalline GaP, the crystalline GaP/adhesive interface, the adhesive/crystalline silicon interface, and the bottom surface of crystalline silicon because of the transparent property of crystalline silicon.

Table II shows a summary of experimental  $A_{\text{eff}}$  for samples with structures of Si/188-nm-thick IGZO/adhesive/188-nm-thick IGZO/Ge, GaAs/130-nm-thick IGZO/adhesive/130-nm-thick IGZO/Si, GaP/102-nm-thick IGZO/adhesive/102-nm-thick IGZO/Si, Si/adhesive/Ge, GaAs/adhesive/Si, and GaP/adhesive/Si. All the samples with IGZO anti-reflection layers gave high  $A_{\text{eff}}$  values of 0.925, 0.943, and 0.931, respectively, compared with 0.751, 0.811, and 0.796 of the simple stacked samples with no IGZO. Although the wavelength gap between  $\lambda_1$  and  $\lambda_2$  was large for Si/188-nm-thick IGZO/adhesive/188-nm-thick IGZO/Ge and GaP/102-nm-thick IGZO/adhesive/102-nm-thick IGZO/Si, the IGZO layers effectively reduced optical reflection, which resulted in high values in  $A_{\text{eff}}$ .

Figure 6 shows calculated  $A_{\text{eff}}$  as a function of IGZO thickness for the three kinds of stacked samples. Experimental results shown in Table II are also plotted.  $A_{\text{eff}}$  increased as the IGZO thickness increased for each sample. It peaked and then decreased as the IGZO thickness further increased. The zero thickness of IGZO was the control sample, which gave the lowest  $A_{\text{eff}}$ . It means that the control sample had the highest optical reflection loss at the intermediate adhesive layer. In particular, the  $A_{\text{eff}}$  of crystalline silicon/adhesive/crystalline germanium was the lowest among the three samples because of the highest refractive index of crystalline germanium, as shown in Fig. 3 and the highest difference in the refractive index between germanium and the adhesive. On the other hand, the control sample of stacking GaAs and silicon gave the highest  $A_{\text{eff}}$ . Although the refractive index of GaAs was higher than that of GaP, the refractive index of silicon markedly increased as the wavelength decreased. The small difference in the refractive index between silicon and the adhesive at wavelength between 902 to 1020 nm resulted in the highest  $A_{\text{eff}}$  among the three control samples.  $A_{\text{eff}}$  increased as the IGZO thickness increased and peaked at the IGZO thicknesses of 183, 130, and 102 nm in the cases of stacking silicon and germanium, GaAs and silicon, and GaP and silicon, respectively. The peaks of  $A_{\text{eff}}$  were higher than 0.9 in all the samples. The maximum  $A_{\text{eff}}$  was 0.95 at  $d$  of 130 nm in the stacked GaAs and silicon because the anti-reflection condition was effectively established in the narrow wavelength width between  $\lambda_1$  (902 nm) and  $\lambda_2$  (1020 nm). The large wavelength width of  $\lambda_1$  and  $\lambda_2$  results in low maximum  $A_{\text{eff}}$ , observed in stacked silicon and germanium, because  $\lambda_1$  (1150 nm) and  $\lambda_2$  (1600 nm) are far different from

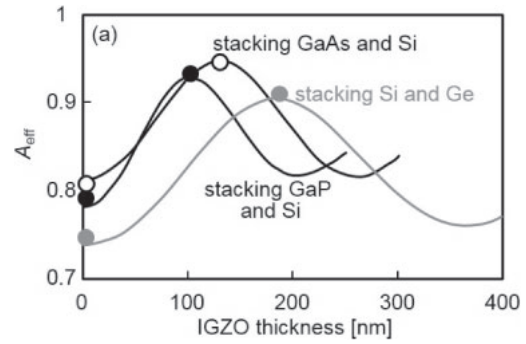


**Fig. 6.** Calculated  $A_{\text{eff}}$  as a function of IGZO thickness of the samples of Si/IGZO/adhesive/IGZO/Ge, GaAs/IGZO/adhesive/IGZO/Si, and GaP/IGZO/adhesive/IGZO/Si. The experimental results shown in Table II are indicated by circles.

$\lambda_{\text{eff}}$  (1356 nm) and the anti-reflection effect is weak at  $\lambda_1$  and  $\lambda_2$  under the best anti-reflection condition at  $\lambda_{\text{eff}}$ .  $A_{\text{eff}}$  gradually decreased as the IGZO thickness further increased after reaching the peak because the anti-reflection condition shifted to wavelengths longer than  $\lambda_{\text{eff}}$ . Although the maximum experimental  $A_{\text{eff}}$  well agreed with that of calculated  $A_{\text{eff}}$  in GaAs/IGZO/adhesive/IGZO/Si and GaP/IGZO/adhesive/IGZO/Si, the maximum experimental  $A_{\text{eff}}$  was slightly higher than that of calculated  $A_{\text{eff}}$  in Si/IGZO/adhesive/IGZO/Ge. The refractive index of the adhesive was probably lower than 1.47 in the experimental samples. The low refractive index of the adhesive reduced the optical reflection at the adhesive region furthermore. In general, the matching condition among the refractive indexes of the semiconductor ( $n_s$ ), IGZO ( $n$ ), and the intermediate adhesive ( $n_a$ ) is given as

$$n = \sqrt{n_s n_a}. \quad (4)$$

The best anti-reflection is given by a low  $n_a$  close to 1.0 for the range of  $n_s$  shown in Fig. 3. An air-gap intermediate connection would be best. The expected  $A_{\text{eff}}$  are 0.975, 0.997, and 0.959 for stacked silicon and germanium, GaAs and silicon, and GaP and silicon with an air gap, respectively. Investigation of adhesive materials with low refractive indices is necessary to achieve high  $A_{\text{eff}}$ . Selection of an anti-reflection layer with a higher refractive index than that of IGZO will possibly lead to the achievement of the condition of Eq. (4). Transparent conductive materials with high refractive indices such as zinc oxide will be candidates for use as the anti-reflection layer.

In this paper, we discussed the reduction of optical reflection loss at the intermediate adhesive region for mechanically stacked samples under the constant-light-intensity spectrum as a function of wavelength. If the spectrum intensity changes with wavelength, for example the air mass 1.5 light spectrum, the equation of  $A_{\text{eff}}$  should be changed by including the light spectrum. Furthermore, the photon flux transmission ratio at the intermediate adhesive region obtained by the modification of Eq. (1) is also important for discussing the photoinduced current density. The current matching condition is mandatorily required for operating multijunction solar cells with high performance because the total current of serially connected multijunction solar cells is limited by the lowest photoinduced current of a cell component. This reduction of optical reflection loss will be important at the intermediate adhesive region for keeping photo-induced current high. If

the photo-induced current density of the bottom cell is critical, it should be increased by better index matching with Eq. (4) as discussed above.

## 5. Conclusions

We demonstrated the reduction of optical reflection loss by IGZO-anti-reflection layers with a refractive index of 1.85 at the intermediate adhesive layer in the visible and infrared regions for mechanically stacked multijunction solar cells. Three kinds of stacked samples with structures of Si/188-nm-thick IGZO/adhesive/188-nm-thick IGZO/Ge, GaAs/130-nm-thick IGZO/adhesive/130-nm-thick IGZO/Si, and GaP/102-nm-thick IGZO/adhesive/102-nm-thick IGZO/Si were fabricated using 6 wt% ITO particles dispersed in the epoxy adhesive with a refractive index of 1.47 by the sputtering method for IGZO formation. The Si/188-nm-thick IGZO/adhesive/188-nm-thick IGZO/Ge sample showed low optical reflectivities ranging from 38.6 to 36.4% at wavelengths ranging from 1150 to 1600 nm, where the top silicon is transparent and the bottom germanium is opaque. The GaAs/130-nm-thick IGZO/adhesive/130-nm-thick IGZO/Si sample showed low optical reflectivities ranging from 33.4 to 33.9% at wavelengths ranging from 902 to 1020 nm. The GaP/102-nm-thick IGZO/adhesive/102-nm-thick IGZO/Si also showed low optical reflectivities ranging from 35.6 to 32.5% at wavelengths ranging from 568 to 1020 nm. Those values were lower than those of simple stacked samples with no IGZO layers. These results experimentally demonstrated that the IGZO layer has the anti-reflection effect at the intermediate adhesive region. The three stacked samples with the IGZO anti-reflection layers described above gave high effective optical absorbency,  $A_{\text{eff}}$ , of the bottom substrates of 0.925, 0.943, and 0.931. Numerical analysis of the optical reflectivity spectra gave the best IGZO thicknesses of 183, 130, and 102 nm for the highest  $A_{\text{eff}}$  for the three kinds of the samples.

## Acknowledgments

This work was supported by the New Energy and Industrial Technology Development Organization (NEDO) and Sameken Co., Ltd.

- 1) W. Shockley and H. J. Queisser, *J. Appl. Phys.* **32**, 510 (1961).
- 2) J. Zhao, A. Wang, M. A. Green, and F. Ferrazza, *Appl. Phys. Lett.* **73**, 1991 (1998).
- 3) A. V. Shah, H. Schade, M. Vanecek, J. Meier, E. Vallat-Sauvain, N. Wyrsh, U. Kroll, C. Droz, and J. Bailat, *Prog. Photovoltaics* **12**, 113 (2004).
- 4) O. Schultz, S. W. Glunz, and G. P. Willeke, *Prog. Photovoltaics* **12**, 553 (2004).
- 5) T. Saga, *NPG Asia Mater.* **2**, 96 (2010).
- 6) H. Sugiura, C. Amano, A. Yamamoto, and M. Yamaguchi, *Jpn. J. Appl. Phys.* **27**, 269 (1988).
- 7) J. M. Olson, S. R. Kurtz, A. E. Kibbler, and P. Faine, *Appl. Phys. Lett.* **56**, 623 (1990).
- 8) M. Tanaka, M. Taguchi, T. Matsuyama, T. Sawada, S. Tsuda, S. Nakano, H. Hanafusa, and Y. Kuwano, *Jpn. J. Appl. Phys.* **31**, 3518 (1992).
- 9) K. A. Bertness, S. R. Kurtz, D. J. Friedman, A. E. Kibbler, C. Kramer, and J. M. Olson, *Appl. Phys. Lett.* **65**, 989 (1994).
- 10) T. Takamoto, E. Ikeda, H. Kurita, M. Ohmori, M. Yamaguchi, and M.-J. Yang, *Jpn. J. Appl. Phys.* **36**, 6215 (1997).
- 11) M. Yamaguchi, *Physica E* **14**, 84 (2002).
- 12) M. Yamaguchi, *Sol. Energy Mater. Sol. Cells* **75**, 261 (2003).
- 13) M. Yamaguchi, T. Takamoto, K. Araki, and N. Ekins-Daukes, *Sol. Energy* **79**, 78 (2005).
- 14) T. Takamoto, M. Kaneiwa, M. Imaizumi, and M. Yamaguchi, *Prog. Photovoltaics* **13**, 495 (2005).
- 15) R. R. King, D. C. Law, K. M. Edmondson, C. M. Fetzer, G. S. Kinsey, H. Yoon, R. A. Sherif, and N. H. Karam, *Appl. Phys. Lett.* **90**, 183516 (2007).
- 16) D. Shahrjerdi, S. W. Bedell, C. Ebert, C. Bayram, B. Hekmatshoar, K. Fogel, P. Lauro, M. Gaynes, T. Gokmen, J. A. Ott, and D. K. Sadana, *Appl. Phys. Lett.* **100**, 053901 (2012).
- 17) H. Mizuno, K. Makita, and K. Matsubara, *Appl. Phys. Lett.* **101**, 191111 (2012).
- 18) H. Mizuno, K. Makita, T. Sugaya, R. Oshima, Y. Hozumi, H. Takato, and K. Matsubara, *Jpn. J. Appl. Phys.* **55**, 025001 (2016).
- 19) G. Flamand and J. Poortmans, *III-Vs Rev.* **19**, 24 (2006).
- 20) M. A. Steiner, J. F. Geisz, J. S. Ward, I. García, D. J. Friedman, R. R. King, P. T. Chiu, R. M. France, A. Duda, W. J. Olavarria, M. Young, and S. R. Kurtz, *IEEE J. Photovoltaics* **6**, 358 (2015).
- 21) T. Ameri, G. Dennler, C. Lungenschmied, and C. J. Brabec, *Energy Environ. Sci.* **2**, 347 (2009).
- 22) S. Wenger, S. Seyrling, A. N. Tiwari, and M. Grätzel, *Appl. Phys. Lett.* **94**, 173508 (2009).
- 23) T. Sameshima, J. Takenezawa, M. Hasumi, T. Koida, T. Kaneko, M. Karasawa, and M. Kondo, *Jpn. J. Appl. Phys.* **50**, 052301 (2011).
- 24) S. Yoshidomi, M. Hasumi, T. Sameshima, K. Makita, K. Matsubara, and M. Kondo, Proc. 6th Thin Film Materials and Devices Meet., 2012, p. 130222027.
- 25) S. Yoshidomi, J. Furukawa, M. Hasumi, and T. Sameshima, *Energy Procedia* **60**, 116 (2014).
- 26) S. Yoshidomi, M. Hasumi, and T. Sameshima, *Appl. Phys. A* **116**, 2113 (2014).
- 27) S. Yoshidomi, S. Kimura, M. Hasumi, and T. Sameshima, *Jpn. J. Appl. Phys.* **54**, 112301 (2015).
- 28) K. Nomura, H. Ohta, A. Takagi, T. Kamiya, M. Hirano, and H. Hosono, *Nature* **432**, 488 (2004).
- 29) J. H. Na, M. Kitamura, and Y. Arakawa, *Appl. Phys. Lett.* **93**, 063501 (2008).
- 30) T. Kamiya, K. Nomura, and H. Hosono, *J. Disp. Technol.* **5**, 273 (2009).
- 31) S. Walheim, E. Schäffer, J. Mlynek, and U. Steiner, *Science* **283**, 520 (1999).
- 32) H. A. Macleod, *Thin-Film Optical Filters* (IOP Publishing, Bristol, U.K., 2001) 3rd ed., Chap. 3, p. 87.
- 33) E. D. Palik, *Handbook of Optical Constants of Solids* (Academic Press, Orlando, FL, 1985) Subpart 2.
- 34) T. Sameshima, H. Hayasaka, and T. Haba, *Jpn. J. Appl. Phys.* **48**, 021204 (2009).
- 35) T. Sameshima, T. Nagao, S. Yoshidomi, K. Kogure, and M. Hasumi, *Jpn. J. Appl. Phys.* **50**, 03CA02 (2011).
- 36) T. Sameshima, K. Betsuin, T. Mizuno, and N. Sano, *Jpn. J. Appl. Phys.* **51**, 03CA04 (2012).
- 37) T. Sameshima, R. Ebina, K. Betsuin, Y. Takiguchi, and M. Hasumi, *Jpn. J. Appl. Phys.* **52**, 011801 (2013).
- 38) T. Sameshima, J. Furukawa, and S. Yoshidomi, *Jpn. J. Appl. Phys.* **52**, 041303 (2013).
- 39) T. Sameshima, J. Furukawa, T. Nakamura, S. Shigeno, T. Node, S. Yoshidomi, and M. Hasumi, *Jpn. J. Appl. Phys.* **53**, 031301 (2014).
- 40) M. Hasumi, T. Nakamura, S. Yoshidomi, and T. Sameshima, *Jpn. J. Appl. Phys.* **53**, 05FV05 (2014).
- 41) T. Sameshima, K. Saitoh, M. Sato, A. Tajima, and N. Takashima, *Jpn. J. Appl. Phys.* **36**, L1360 (1997).
- 42) T. Sameshima, K. Saitoh, N. Aoyama, M. Tanda, M. Kondo, A. Matsuda, and S. Higashi, *Sol. Energy Mater. Sol. Cells* **66**, 389 (2001).
- 43) K. Ukawa, Y. Kanda, T. Sameshima, N. Sano, M. Naito, and N. Hamamoto, *Jpn. J. Appl. Phys.* **49**, 076503 (2010).
- 44) M. Born and E. Wolf, *Principle of Optics* (Pergamon, New York, 1974) Chaps. 1 and 13.